A DFT study of the unusual substrate-assisted mechanism of Serratia marcescens chitinase B reveals the role of solvent and mutational effect on catalysis

ARTICLE *in* JOURNAL OF MOLECULAR GRAPHICS AND MODELLING · DECEMBER 2014

Impact Factor: 1.72 · DOI: 10.1016/j.jmgm.2014.12.002

4 AUTHORS:

Jitrayut Jitonnom

University of Phayao

15 PUBLICATIONS **67** CITATIONS

SEE PROFILE

Chanchai Sattayanon

Chiang Mai University

4 PUBLICATIONS **7** CITATIONS

SEE PROFILE

Nawee Kungwan

Chiang Mai University

55 PUBLICATIONS **217** CITATIONS

SEE PROFILE

Supa Hannongbua

Kasetsart University

175 PUBLICATIONS **1,382** CITATIONS

SEE PROFILE

Journal of Molecular Graphics and Modelling 56 (2015) 53–59

Contents lists available at ScienceDirect

Journal of Molecular Graphics and Modelling

journal homepage: www.elsevier.com/locate/JMGM

A DFT study of the unusual substrate-assisted mechanism of *Serratia marcescens* chitinase B reveals the role of solvent and mutational effect on catalysis

Jitrayut Jitonnom[a,*], Chanchai Sattayanon[b], Nawee Kungwan[b], Supa Hannongbua[c]

[a] Division of Chemistry, School of Science, University of Phayao, Phayao 56000, Thailand
[b] Department of Chemistry, Faculty of Science, Chiang Mai University, Chiang Mai 50200, Thailand
[c] Department of Chemistry, Faculty of Science, Kasetsart University, Bangkok 10900, Thailand

ARTICLE INFO

Article history:
Accepted 8 December 2014
Available online 16 December 2014

Keywords:
DFT
Glycoside hydrolase
Chitinase B
Enzyme reaction
Substrate-assisted catalysis
Mutation

ABSTRACT

Serratia marcescens chitinase B (SmChiB) catalyzes the hydrolysis of β-1,4-glycosidic bond, via an unusual substrate-assisted mechanism, in which the substrate itself acts as an intramolecular nucleophile. In this paper, the catalytic mechanism of SmChiB has been investigated by using density functional theory. The details of two consecutive steps (glycosylation and deglycosylation), the structures and energetics along the whole catalytic reaction, and the roles of solvent molecules as well as some conserved SmChiB residues (Asp142, Tyr214, Asp215, and Arg294) during catalysis are highlighted. Our calculations show that the formation of the oxazolinium cation intermediate in the glycosylation step was found to be a rate-determining step (with a barrier of 23 kcal/mol), in line with our previous computational studies (Jitonnom et al., 2011, 2014). The solvent water molecules have a significant effect on a catalytic efficiency in the degycosylation step: the catalytic water is essentially placed in a perfect position for nucleophic attack by hydrogen bond network, lowering the barrier height of this step from 11.3 kcal/mol to 2.9 kcal/mol when more water molecules were introduced. Upon the *in silico* mutations of the four conserved residues, their mutational effects on the relative stability of the reaction intermediates and the computed energetics can be obtained by comparing with the wild-type results. Mutations of Tyr214 to Phe or Ala have shown a profound effect on the relative stability of the oxazolinium intermediate, emphasizing a direct role of this residue in destabilizing the intermediate. In line with the experiment that the D142A mutation leads to almost complete loss of SmChiB activity, this mutation greatly decreases the stability of the intermediate, resulting in a very large increase in the activation barrier up to 50 kcal/mol. The salt-bridges residues (Asp215 and Arg294) were also found to play a role in stabilizing the oxazolinium intermediate.

1. Introduction

Serratia marcescens chitinase B (SmChiB), belonging to the glycosidase family 18, degrades chitin (an insoluble linear polymer of β-(1,4)-linked *N*-acetylglucosamine $(GlcNAc)_n$) which is the second most abundant biopolymer in nature after cellulose. SmChiB has received much attention as an attractive system for the development of new inhibitors with chemotherapeutic potential [1,2]. It has also been applied in biotechnology for conversion of insoluble polysaccharides into commercially valuable product [3,4]. SmChiB has been suggested experimentally [5] and theoretically [6–8] to catalyze the hydrolysis of β-1,4-glycosidic bonds found in chitin, via an unusual substrate-assisted mechanism (see Fig. 1). In brief, SmChiB catalyzed the glycosidic bond hydrolysis via a two-step mechanism in which the formation of oxazolinium intermediate takes place in the first step (glycosylation), followed by hydrolysis of the intermediate in the second step (deglycosylation), yielding the sugar product with retention of configuration at the anomeric center. After catalytic reaction, the product is then released from the substrate binding cleft of SmChiB which is suggested to proceed via the unbinding event [6].

The catalytic function of this enzyme has been found to depend on a relatively large number of residues [9]. Asp140, Asp142 and Glu144, conserved in most family 18 chitinases, form a catalytic triad in the active site of SmChiB. Glu144 is known to act as a catalytic acid/base [5]. Asp142, together with Asp140, are suggested

* Corresponding author. Tel.: +66 05446 6666x1834; fax: +66 05446 6664.
E-mail address: jitrayut.018@gmail.com (J. Jitonnom).

http://dx.doi.org/10.1016/j.jmgm.2014.12.002
1093-3263/

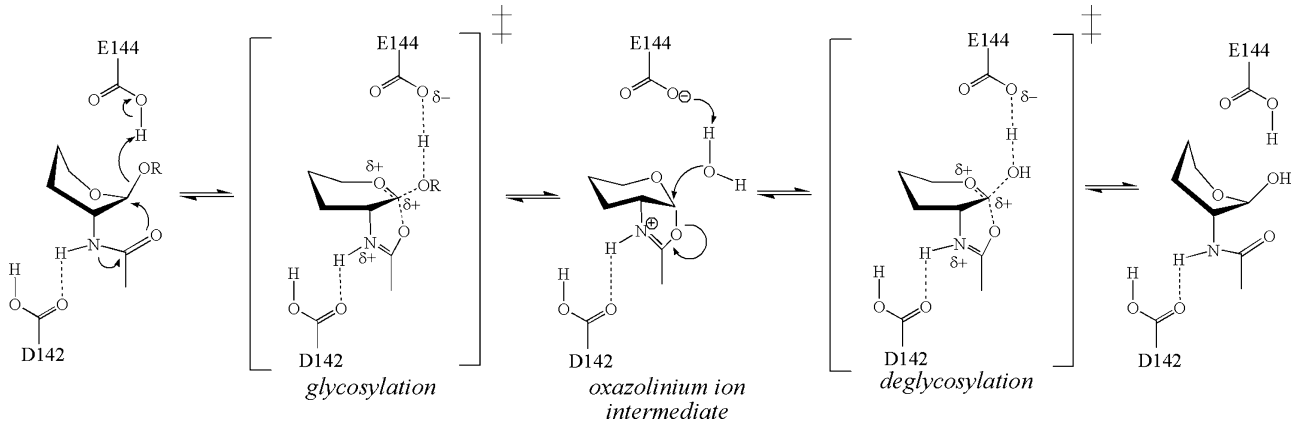

Fig. 1. Schematic presentation of substrate-assisted (retaining) mechanism of *Serratia marcescens* ChiB (SmChiB).

to be involved in binding of substrate [9] and catalysis [6,7]. Other conserved residues (e.g., Tyr10, Ser93, Tyr214, Asp215 and Arg294) have also been found to influence the catalytic activity of the enzyme [9]. Among these, Asp142, Tyr214 and a salt-bridge (Asp215 and Arg294) are of particular interest as they are located at the catalytic center of SmChiB and participate directly to the binding of substrate at subsites −1 and +1, in cooperation with other hydrophobic residues including Trp97, Trp220, and Trp403 (see Fig. 2). Moreover, Tyr214, in conjunction with Asp142 and Asp215, is proposed to interact with the substrate upon binding and has been observed to contribute to the distortion of the *N*-acetyl group on the −1 sugar [5,9]. In addition to their role in substrate binding, they have been proved to be critical for SmChiB catalysis: Asp142 has been found, in its neutral protonation state, to be important in stabilizing the transition state and the intermediate, by electrostatic interactions [6,7]. Recently, Tyr214 has been shown by our group to play a critical role in the deglycosylation step of the reaction, by destabilizing the intermediate via its H-bond formed with the substrate [6] and thus lowering the energy barrier in this step by about 8.5 kcal/mol. Similar role of analogous tyrosine was also found in GH1 beta-glucosidase [10]. Meanwhile, the role of the Asp215 and Arg294 salt-bridge is likely to contribute electrostatically to the reaction. While the catalytic role of these residues seems to be well described, it is of particular importance to probe the influence of these residues on each individual step of SmChiB reaction.

To further investigate the roles of these conserved residues (Asp142, Tyr214, Asp215 and Arg294) and in particular their fundamental impact on energetics of each individual step of the SmChiB reaction, a theoretical study on the catalytic mechanism of SmChiB with hybrid density functional theory (DFT) method has been carried out to provide structural information of intermediates and energetics along the whole catalytic reaction of wild-type SmChiB. Upon the wild-type geometry, several mutants corresponding to those four conserved residues (see Fig. 2) were *in silico* made and their computed energetics was then obtained for comparison with the wild-type results. In addition, we also modeled different number of water molecules in the second half of the reaction and have demonstrated the role of solvent during chitin hydrolysis.

2. Computational details

The initial structure of the enzyme–substrate (ES) complex was taken from the X-ray structure (PDB entry 1E6N) [5] of the E144Q mutant of *S. marcescens* ChiB with a chitopentaose $(GlcNAc)_5$ substrate bound along subsites −2 to +3 (see Fig. 2). The wild-type was recovered by manually altering Gln144 to Glu144. The enzyme active site was truncated via Cβ carbon atoms, generating a quantum cluster model of ES for the first (glycosylation) step that consists of side-chain atoms of Asp142, Glu144, Tyr214, Asp215 and Arg294 and one chitobiose molecule (occupying at GlcNAc subsites −1 and +1). In the next (deglycosylation) step, another cluster

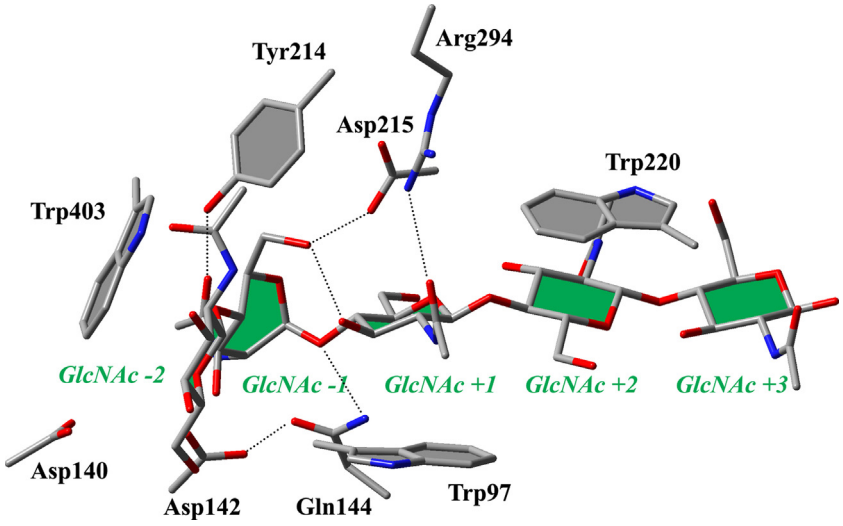

Fig. 2. X-ray structure of the active site of SmChiB complexes with *N*-acteylglucosamine substrate, $(GlcNAc)_5$, (coordinates taken from PDB entry 1E6N).

model (denoted as EI2) was built based on the final geometry of the last step of glycosylation (denoted as EI1) with one chitose molecule occupying at GlcNAc subsite +1 removed. One water molecule was added at a position of leaving group oxygen (O_{gly}), generating a nucleophilic water model (**1wat**). To test the solvent effect on the catalysis, additional water molecules were explicitly added into the EI2 model by gradually placing a water molecule around the (optimized) catalytic water and computing their configurations and energetic. Note that six water molecules were added but only four could maximally be modeled with stationary point found during the geometry optimization. The failure to find the optimized geometry of the higher number of water molecules (i.e., five and six waters) is probably due to the small size of the EI2 model which may not large enough to contain those waters. Finally, four different number of water models were studied and denoted as **1wat**, **2wat**, **3wat** and **4wat**, respectively. All cluster models were subjected to geometry optimizations with zero net charge. The Becke-3-Lee-Yang-Parr (B3LYP) exchange correlation functional and a standard basis set (6–31G(d)) [11] were used. Using quantum chemical cluster calculation, a computational method that has been widely applied in modeling enzymatic reaction [12], the geometries of stationary points were obtained with truncated atoms (Cβ atoms) constraint to their corresponding positions from the X-ray structure, keeping the optimized structures close to those obtained experimentally. Frequencies were calculated at the same level of theory as the geometry optimizations to confirm the nature of the stationary points and also to obtain zero-point energies (ZPE). Since some atoms were frozen to their crystallographic positions, a few small negative eigenvalues usually appear, in this case all below 50i cm^{-1}. These frequencies do not contribute significantly to the ZPE and can be ignored [13,14]. Effects of implicit solvent and protein environment (with the conductor-like polarized continuum model) [15] as well as energy correction at larger basis set (B3LYP/6-311++G(3df,3pd)//B3LYP/6-31G(d)) were also tested on the optimized structures, which give a similar result in terms of relative energetics and mechanism (see Table S1; Supporting Information). The energy profile of glycosylation was calculated using the ES as reference while that of deglycosylation was calculated with respect to the EI2. All calculations reported in this work were performed using Gaussian 09 [16].

3. Results and discussion

In order to understand the mutational effects of the conserved residues on the catalysis of the wild-type SmChiB, all structural and energetic information for the wild-type reaction need to be established as a reference. As mentioned above, the first step (glycosylation) of the reaction involves formation of an oxazolinium intermediate which then collapses upon hydrolysis in the second step (deglycosylation), yielding the sugar product. The detailed information for the two consecutive steps is described as follows.

3.1. Enzyme–substrate complex

The structures and energetic along the glycosylation and deglycosylation paths as calculated by the DFT cluster method at the B3LYP level are shown in Fig. 3. Key structural parameters are summarized in Table 1. Let consider the geometry at the ES complex shown in Fig. 3A. As seen, the quantum cluster model of ES generally represents the geometry observed for the X-ray structure of mutant (E144Q) SmChiB (see Fig. 2 and Table 1). In particular, a twisted glycosidic bond within the $(GlcNAc)_2$ substrate could be maintained through seven hydrogen bonds (**a**–**g**), assisted mainly by several enzyme active site residues, and thus supporting the role of these conserved residues in the substrate binding. Asp142, Glu144 and Tyr214 are fully responsible for the substrate distortion: the two carboxyl residues form a strong hydrogen-bonding network (see distances **a**, **b** and **g**) that essentially places the substrate in a reactive orientation while Tyr214 helps the two residues in twisting the *N*-acetyl group of the −1 GlcNAc via a hydrogen bond (distance **c**). This distortion facilitates a decrease in the C1—O_{NAc} distance involved in the intramolecular nucleophilic attack and thus helps to promote the formation of oxazolinium intermediate in the first step (glycosylation) of the SmChiB reaction.

3.2. Glycosylation path

As shown schematically in Fig. 1, the glycosylation step is the formation of an oxazolinium cation intermediate where two chemical processes are involved, that is, the proton transfer from Glu144 proton to the scissile glycosidic oxygen (see ***a***; O_{gly}—HO(Glu144)) and the nucleophilic addition of the *N*-acetyl oxygen at the anomeric C1 carbon (C1—O_{NAc}). Our DFT models indicate that these two processes occur simultaneously in an asynchronous manner. Starting from ES to TS1, Glu144 completely donates its proton to the glycosidic oxygen (see ***a***; O_{gly}—HO(Glu144) = 1.10 Å), activating the cleavage of glycosidic bond. At the same time, the scissile glycosidic bond (O_{gly}—C1) is elongated (1.48 Å at ES to 2.27 Å at TS1) and the C1—O_{NAc} distance between the anomeric carbon (C1) and the *N*-acetyl oxygen (O_{NAc}) becomes shorter (3.08 Å at ES to 2.29 Å at TS1). At this stage, the −1 GlcNAc ring was found to adopt a coplanar geometry (0.6°) between atoms C3, C2, C1 and O_{ring}, featuring a $^4H_5$ half-chair conformation, which is in agreement to our previous observations [6,7]. Upon the cleavage of the glycosidic bond, the intramolecular nucleophilic attack takes place in a synchronous process, resulting in a narrowing of the *N*-acetyl oxygen and the anomeric carbon distance and the formation of the bicyclic structure of the oxazolinium intermediate, which is characterized by an intramolecular covalent bond formed (C1—O_{NAc} = 1.57 Å) inside the sugar at the EI1. The glycosylation step is endothermic by 11 kcal/mol with a calculated activation energy of 23.0 kcal/mol (see Fig. 3B). The conformation itinerary adopted by the GlcNAc moiety at the subsite−1 of this step is also depicted in Fig. 3B, which is found to follow a boat $(^{1,4}B) \rightarrow$ a half-chair $(^4H_5)^{\ddagger} \rightarrow$ chair $(^4C_1)$ pattern.

3.3. Deglycosylation path

The second step (deglycosylation) of the reaction requires an essential water molecule near the anomeric carbon (C1) to act as a nucleophile during the breakdown of the intermediate formed in the first step. In our previous study, we found that there are at least three water molecules participating in a near-attack position close to the C1 atom during the 1 ns QM/MM MD simulation of enzyme-intermediate complex (EI2) [6]. However, only one water molecule having the best positioning for nucleophilic attack was chosen to be treated quantum mechanically in the QM/MM reaction modeling. Here we included more water molecules explicitly in our cluster model. The higher number of water molecules was modeled to understand the role of the solvent on the catalytic efficiency of the SmChiB enzyme, which is often ignored in most theoretical studies of glycosidase reaction [6,7,10,17–23]. Representative structures and energetics along the deglycosylation path with one to three water molecules modeled (**1wat**, **2wat** and **3wat**) are shown in Fig. 4. This step is represented by the **2wat** model as this is a minimum model that could produce a water nucleophile in a perfect position for reaction and its geometric parameter is included in Table 1. Additional geometric parameters for the remaining water models are summarized in the Supporting Information (Table S2).

In an opposite direction to the first step, the second step is initiated by nucleophilic attack of the catalytic water at the anomeric

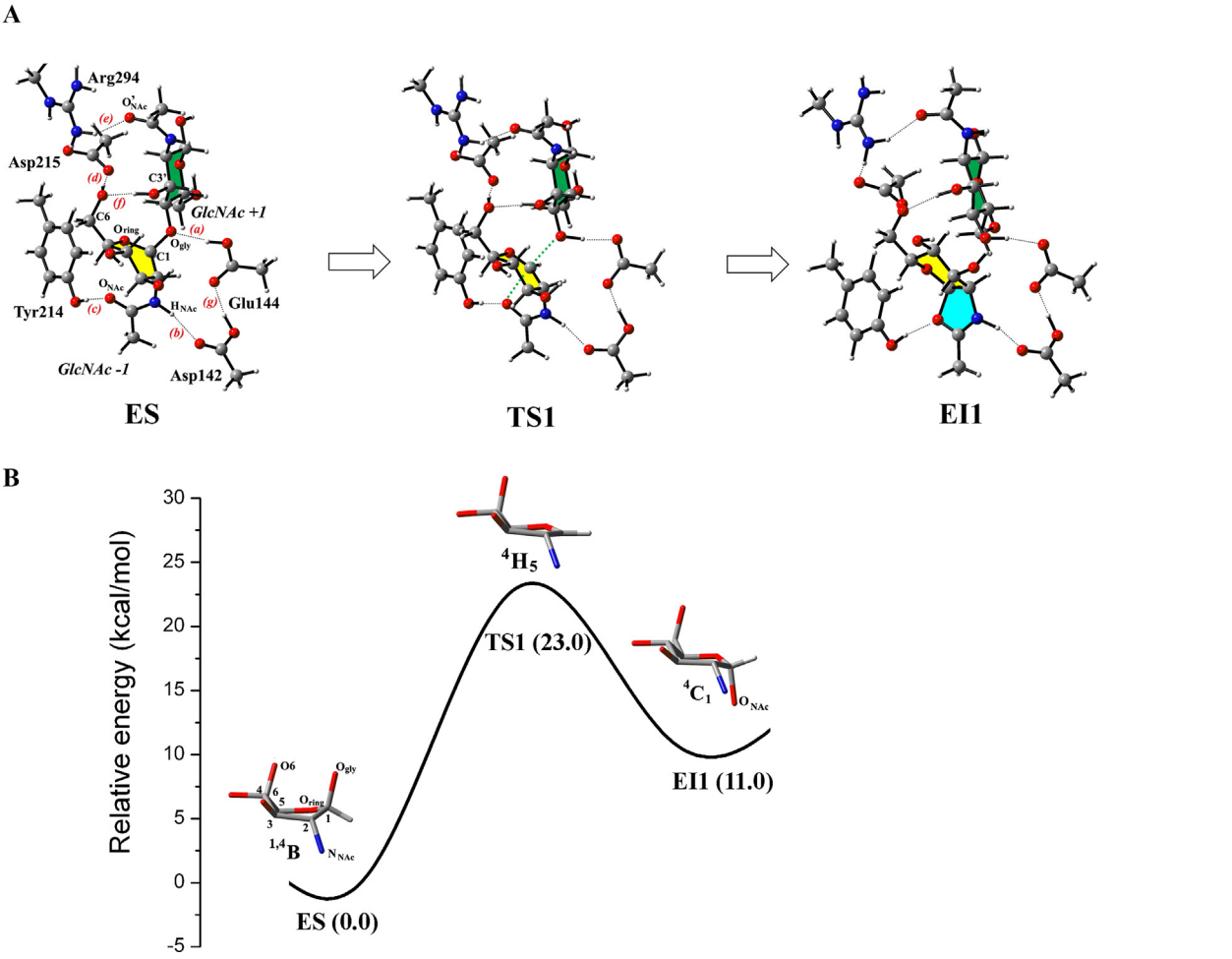

Fig. 3. Structures (A) and energetic (B) along the glycosylation path of SmChiB reaction. Conformation of the −1 GlcNAc is also included with some hydrogen atoms are omitted for clarity.

center, following by the collapse of the intermediate (EI2) and the subsequent formation of the reaction product (EP) as shown in Fig. 4A. At TS2, the catalytic water was found to be positioned close to the anomeric carbon (C1—O_{wat}; 2.88 Å (EI2) → 2.42 Å (TS2)) while the fused oxazoline ring is spontaneously broken (C1—O_{NAc}; 1.55 Å (EI2) → 2.14 Å (TS2)). A fully bonded O_{wat}—H_{wat} distance of 1.01 Å at TS2 indicates that no proton abstraction occurs at this stage, that is, the transfer of a proton from the catalytic water onto the Glu144 residue does not occur, in agreement to our previous observation [6]. After TS2, the proton abstraction was achieved with the fully H_{wat}—O(Glu144) bonded distance of 1.00 Å, resulting in the formation of the EP and a subsequent release of the product, which is

Table 1
Selected structural parameters (interatomic distances and angles) of the stationary points on the potential energies of glycosylation and deglycosylation paths.

Distance (Å), angle (°)	Expt[a]	Glycosylation			Deglycosylation (**2wat**)		
		ES	TS1	EI1	EI2	TS2	EP
O_{gly}—C1	1.39	1.48	2.27	2.87	–	–	–
C1—O_{NAc}	2.98	3.08	2.29	1.57	1.56	2.14	2.96
O_{gly}—HO(Glu144) (a)	3.19[b]	1.90	1.10	0.99	–	–	–
C1—O_{ring}	1.45	1.38	1.28	1.34	1.34	1.28	1.38
O_{wat}—C1	–	–	–	–	2.92	2.42	1.46
H_{wat}—O(Glu144)	–	–	–	–	1.78	1.59	0.99
O_{wat}—H_{wat}	–	–	–	–	0.98	1.02	1.86
H_{NAc}—O(Asp142) (b)	2.89[c]	2.01	1.79	1.55	1.54	1.84	2.08
O_{NAc}—HO(Tyr214) (c)	2.66[b]	1.80	1.91	2.13	2.04	1.86	1.77
C6OH—O(Asp215) (d)	2.64[b]	1.61	1.59	1.65	1.72	1.64	1.67
O'_{NAc}—HN(Arg294) (e)	3.09[c]	1.95	1.90	1.93	–	–	–
C6:HO—HO:C3′ (f)	2.61[b]	1.71	1.79	1.81	–	–	–
O(Glu144)—HO(Asp142) (g)	2.71[b]	1.74	1.43	1.05	1.50	1.46	1.74
C3—C2—C1—O_{ring}	−41.0	−33.0	0.6	26.4	26.5	12.1	−16.3

[a] Values taken from the experimentally determined X-ray structure of E144Q mutant ChiB (PDB entry 1E6N, chain A) from Ref. [5].
[b] O—O distance.
[c] N—O distance.

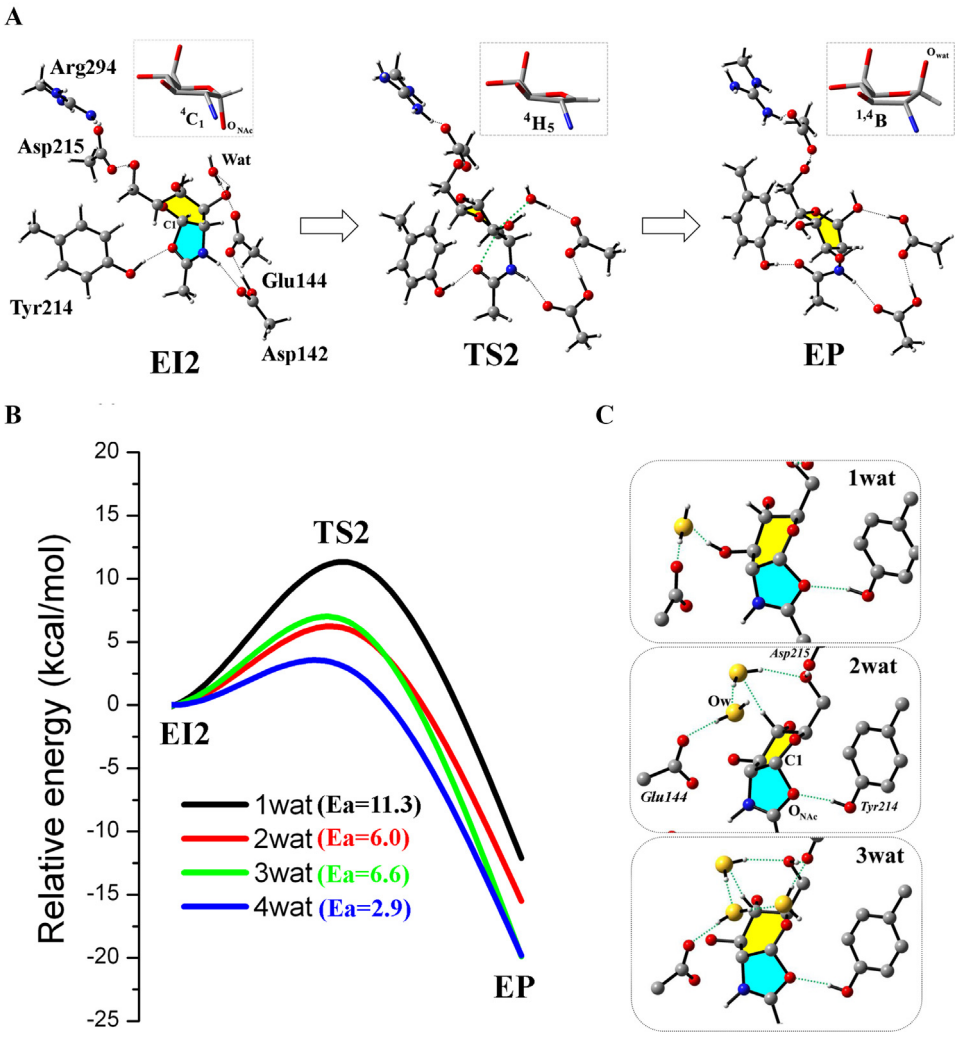

Fig. 4. Representative structures (A) and energetic (B) along the deglycosylation path of SmChiB reaction with different number of water molecules modeled near C1 atom. Initial optimized structures of EI2 (C) for **1wat**, **2wat** and **3wat** are demonstrated with oxygen atoms colored in yellow. (For interpretation of the references to colour in this figure legend, the reader is referred to the web version of this article.)

proposed to be triggered by the rotation of Asp142 side chain in concomitant with the flip of the *N*-acetyl group of subsite −1 NAG [6].

In this deglycosylation, a reverse conformations of the −1 GlcNAc sugar was found as chair ($^4C_1$) → half-chair [$^4H_5$]‡ → boat ($^{1,4}B$).

As shown in Fig. 4B, the barrier height of the second step was significantly decreased (from 11.3 kcal/mol to 2.9 kcal/mol) when more number of water molecules were introduced in the model system, emphasizing the essential role of water molecules for efficient catalysis. While all model systems seem to have a similar geometry, a minor difference for the position of the water nucleophile is still seen at the EI2 (see Fig. 4C) where a hydrogen bond (H-bond) network playing a role. As shown, a large barrier (11.3 kcal/mol) observed at TS2 of **1wat** is observed due to a weak H-bond stabilization provided by water molecules. On the other hand, increasing number of water molecules (for either **2wat** or **3wat** models) appears to create more H-bond network and helps in positioning the nucleophile water in a perfect position for reaction, as evident by the shorter C1—O_{wat} distances of 2.92 Å (**2wat**) and 2.87 Å (**3wat**) compared to that (4.45 Å) in **1wat**. Thus, the more water molecules would provide a stronger H-bond stabilization that leads to a lower energy barrier in the deglycosylation step. In addition, they also contribute to the product stability (see Fig. S1 in the Supporting Information).

The lower energy barriers for the second step (in range of 11.3–2.9 kcal/mol relative to the EI2) comparing to that (23.0 kcal/mol) for the first step (Fig. 3B) suggest that the glycosylation path is the rate-determining step of the overall reaction of SmChiB.

3.4. Energetic analysis of mutants

To further understand the mutational effect on the energetic along both glycosylation and deglycosylation pathways, several *in silico* mutations were made based on the geometry of the optimized structure of the wild-type SmChiB. We selected the **2wat** system as a representative model of the second step for energetic analysis of mutants.

3.4.1. Y214F

Our previous simulation [6] has shown that the Tyr214 residue could adopt two orientations, corresponding to the different H-bond interaction formed between the OH-group of Tyr214 and the oxazoline ring within the intermediate, and we found that this H-bond is essential for an efficient deglycosylation step in the SmChiB

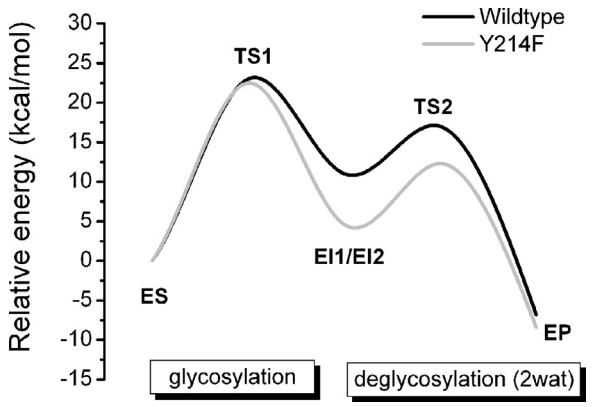

Fig. 5. Relative potential energy profiles for overall reaction in wild-type (black) and Y214F mutant (grey) SmChiB based on the two waters model (**2wat**) system.

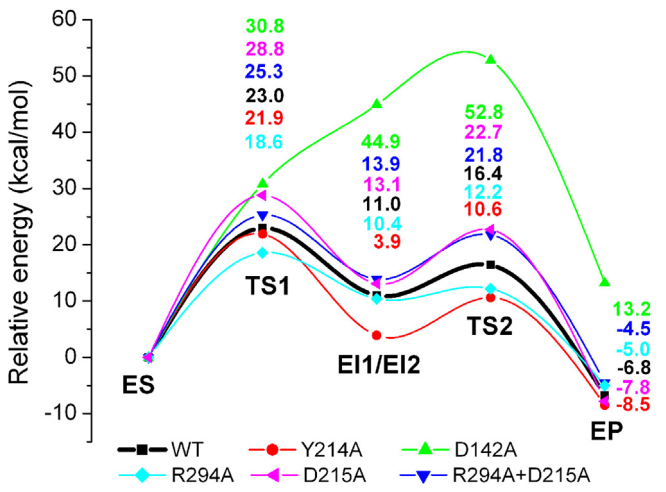

Fig. 6. Relative potential energy profiles for both glycosylation and deglycosylation paths of SmChiB reaction for wild-type (black) and other alanine mutations.

reaction, which provides explanation to the origin of the reduced rate observed in the Y214F mutant observed in the experiment, as well as its analogous residue in other GH enzymes [24–26]. However, this conclusion was drawn based on energetic analysis of the wild-type, not the Y214F mutant, that does not account for the electronic effect of the Tyr214 residue (as this residue was treated classically during the simulation), which provides only an indirect implication to the reduced rate of Y214F mutant. Here, the electronic effect of Tyr214 is fully described and the Y214F mutant was generated based on *in silico* mutation of the optimized geometry of the wild-type SmChiB. Calculated reaction energetics for each individual step of the mutant is shown in Fig. 5, in comparison with the energy profile of the wild-type. Clearly, the Y214F mutant causes only a small effect on the glycosylation step with a slightly lower barrier at TS1 (22.5 kcal/mol). On the other hand, the mutant has a profound effect on the deglycosylation step, and in particular the relative stability of oxazolinium intermediate (EI1/EI2) formed in the glycosylation step: it stabilizes the intermediate more effectively as indicated by a large decrease in the EI1/EI2 energy from 11.0 kcal/mol in wild-type to 4.1 kcal/mol in Y214F. This result also implies that Tyr214 exhibits a stronger destabilization to the intermediate compared to the Phe residue, as the tyrosine residue polarizes, via its H-bond, the oxazoline ring formed in the glycosylation step, thus facilitating an efficient deglycosylation. More interestingly, the reduction of the EI energy leads to an increase in a barrier height of the deglycosylation step from 6.0 to 8.8 kcal/mol in wild-type and Y214F, respectively. This result was also found in other water models (see Figs. S2 and S3 in the Supporting Information). A similar change of the energy profile was also found in the case of Y214A mutation, as described below. This energetic analysis indicate clearly that the Y214F mutation has a dominant effect on the second step of the reaction, not on the first step, further supporting our recent study of the vital role of Tyr214 in deglycosylation [6] in which the residue plays a role in destabilizing the intermediate via hydrogen bond. This information would also explain why mutations of similar analogous residue (Y217F and Y228A) decreased hydrolytic activities with improved transglycosylation ability in endo-beta-N-acetylglucosaminidases [27] and *Serratia proteamaculans* ChiD [28], respectively.

3.4.2. Other mutants

To further probe the reaction energetic of other mutants, several alanine mutations on residues surrounding the −1 and +1 GlcNAc were performed and their corresponding energetics along the reaction were examined, as shown in Fig. 6. The mutations were involved two single mutations of Asp142 and Tyr214 and a double mutation of Arg294 and Asp215. We found that the Y214A mutation exhibited a similar reaction energy profile to that of the Y214F. Interestingly, D142A was found to be most affected on both energetics and mechanism. Instead of a two-step mechanism the mutant proceed the reaction, via one transition state, that required a very large energy barrier of 52.8 kcal/mol. This result supports our previous observations [7], emphasizing a necessary of the Asp142–Glu144 interaction and their ability to stabilize the oxazolinium cation species electrostatically, leading to a lower reaction barrier. The large barrier generated by the D142A mutation not only reflects a decreased rate of SmChiB hydrolysis, but also provides evidence to support the improved transglycosylation activity observed in variants of Asp-142/313, analogous residues in SmChiB and SmChiA, respectively [27,29]. The salt-bridge residues, Arg294 and Asp215 are likely to give an opposite role. By comparing to that of wild-type reaction, the D215A was attributed to the higher energy barrier for glycosylation and deglycosylation whereas R294A was found to lower the barriers of both steps to 18.6 and 1.8 kcal/mol, respectively. The role of these salt-bridge residues can be further seen from the double mutation which clearly showed an increased barrier for both reaction steps, with the deglycosylation having the most effect. Like Asp142, this salt-bridge was also found to play a role in stabilizing the oxazolinium intermediate as this double mutation gives a higher energy of the EI compared to that of the wild-type.

4. Conclusions

In this study, quantum cluster models with density functional theory are successfully used not only to describe the unusual substrate-assisted mechanism at a molecular level but also to demonstrate the influence of four conserved residues (Asp142, Tyr214, Asp215 and Arg294) at the catalytic center of SmChiB on catalysis. Structural and energetic information of the reaction in wild-type SmChiB were provided by the models, supporting the two-step mechanism involving the formation of an oxazolinium intermediate and the subsequent collapse of the intermediate upon hydrolysis yielding the sugar product. The first step was found to be the rate-determining step of the overall reaction with the calculated activation barrier of 23.0 kcal/mol, in agreement to our previous studies. In the second step, the reaction barrier was found to be lower (from 11.3 kcal/mol to 2.9 kcal/mol) when more water molecules were introduced in the model systems, emphasizing the important role of solvent in catalytic efficiency. By comparing with the wild-type results, the mutational effect of four conserved residues in the SmChiB active site on reaction energetics of each individual step was allowed to be studied. Mutations of Tyr214 to

Phe or Ala have shown a profound effect on the relative stability of the oxazolinium intermediate, which exhibits the decreased EI energy that turns out to raise the energy barrier in the deglycosylation step. This observation has confirmed another important role of Tyr214 residue in intermediate destabilization and deglycosylation activity, besides its role in substrate distortion. The D142A mutation greatly decreases the stability of the intermediate, resulting in a very large increase in the activation barrier up to 50 kcal/mol. The salt-bridges residues (Asp215 and Arg294) were also found to play a role in stabilizing the oxazolinium intermediate. Our modeling approach may be useful as a computational probe to understand the influence of key conserved residues on the individual step of enzyme reaction, complementary to the site-direct mutagenesis experiment.

Acknowledgements

This work was carried out within the Research Grant for New Scholar (Grant no. MRG5680143) that is co-funded by the Thailand Research Fund, the Office of the Higher Education Commission, the University of Phayao. N.K. thanks Chiang Mai University for financial support. J.J. is funded by the University of Phayao (Grants nos. R020056216016 and R020057316004) and thanks the National e-Science Infrastructure Consortium for providing computing resources (http://www.e-science.in.th).

Appendix A. Supplementary data

Supplementary data associated with this article can be found, in the online version, at http://dx.doi.org/10.1016/j.jmgm.2014.12.002.

References

[1] O.A. Andersen, M.J. Dixon, I.M. Eggleston, D.M. van Aalten, Natural product family 18 chitinase inhibitors, Nat. Prod. Rep. 22 (2005) 563–579.
[2] D.R. Houston, B. Synstad, V.G. Eijsink, M.J. Stark, I.M. Eggleston, D.M. van Aalten, Structure-based exploration of cyclic dipeptide chitinase inhibitors, J. Med. Chem. 47 (2004) 5713–5720.
[3] S.J. Horn, P. Sikorski, J.B. Cederkvist, G. Vaaje-Kolstad, M. Soerlie, B. Synstad, et al., Costs and benefits of processivity in enzymatic degradation of recalcitrant polysaccharides, Proc. Natl. Acad. Sci. U. S. A. 103 (2006) 18089–18094.
[4] G. Vaaje-Kolstad, S.J. Horn, M. Sorlie, V.G. Eijsink, The chitinolytic machinery of *Serratia marcescens* – a model system for enzymatic degradation of recalcitrant polysaccharides, FEBS J. 280 (2013) 3028–3049.
[5] D.M.F. Van Aalten, D. Komander, B. Synstad, S. Gaseidnes, M.G. Peter, V.G.H. Eijsink, Structural insights into the catalytic mechanism of a family 18 exo-chitinase, Proc. Natl. Acad. Sci. U. S. A. 98 (2001) 8979–8984.
[6] J. Jitonnom, M.A. Limb, A.J. Mulholland, QM/MM free-energy simulations of reaction in *Serratia marcescens* chitinase B reveal the protonation state of Asp142 and the critical role of Tyr214, J. Phys. Chem. B 118 (2014) 4771–4783.
[7] J. Jitonnom, V.S. Lee, P. Nimmanpipug, H.A. Rowlands, A.J. Mulholland, Quantum mechanics/molecular mechanics modeling of substrate-assisted catalysis in family 18 chitinases: conformational changes and the role of Asp142 in catalysis in ChiB, Biochemistry 50 (2011) 4697–4711.
[8] C.M. Payne, J. Baban, S.J. Horn, P.H. Backe, A.S. Arvai, B. Dalhus, et al., Hallmarks of processivity in glycoside hydrolases from crystallographic and computational studies of the *Serratia marcescens* chitinases, J. Biol. Chem. 287 (2012) 36322–36330.
[9] B. Synstad, S. Gaseidnes, D.M.F. van Aalten, G. Vriend, J.E. Nielsen, V.G.H. Eijsink, Mutational and computational analysis of the role of conserved residues in the active site of a family 18 chitinase, Eur. J. Biochem. 271 (2004) 253–262.
[10] S. Badieyan, D.R. Bevan, C. Zhang, Probing the active site chemistry of beta-glucosidases along the hydrolysis reaction pathway, Biochemistry 51 (2012) 8907–8918.
[11] A.D. Becke, Density-functional thermochemistry III. The role of exact exchange, J. Chem. Phys. 98 (1993) 5648–5652.
[12] P.E. Siegbahn, F. Himo, Recent developments of the quantum chemical cluster approach for modeling enzyme reactions, J. Biol. Inorg. Chem. 14 (2009) 643–651.
[13] K. Wang, Q. Hou, Y. Liu, Insight into the mechanism of aminomutase reaction: a case study of phenylalanine aminomutase by computational approach, J. Mol. Graph. Model. 46 (2013) 65–73.
[14] X. Sheng, Y. Liu, C. Liu, Theoretical studies on the common catalytic mechanism of transketolase by using simplified models, J. Mol. Graph. Model. 39 (2013) 23–28.
[15] M. Cossi, N. Rega, G. Scalmani, V. Barone, Energies, structures, and electronic properties of molecules in solution with the C-PCM solvation model, J. Comput. Chem. 24 (2003) 669–681.
[16] M.J.G.W.T. Frisch, H.B. Schlegel, G.E. Scuseria, M.A.J.R.C. Robb, G. Scalmani, V. Barone, B. Mennucci, G.A.H.N. Petersson, M. Caricato, X. Li, H.P. Hratchian, A.F.J.B. Izmaylov, G. Zheng, J.L. Sonnenberg, M. Hada, M.K.T. Ehara, R. Fukuda, J. Hasegawa, M. Ishida, T. Nakajima, Y.O.K. Honda, H. Nakai, T. Vreven, J.A. Montgomery Jr., et al., Gaussian 09, Revision D.01, 2013.
[17] X. Biarnes, J. Nieto, A. Planas, C. Rovira, Substrate distortion in the Michaelis complex of Bacillus 1,3-1,4-b-glucanase: insight from first principles molecular dynamics simulations, J. Biol. Chem. 281 (2006) 1432–1441.
[18] N.F. Bras, P.A. Fernandes, M.J. Ramos, QM/MM studies on the beta-galactosidase catalytic mechanism: hydrolysis and transglycosylation reactions, J. Chem. Theory Comput. 6 (2010) 421–433.
[19] J. Liu, X. Wang, D. Xu, QM/MM study on the catalytic mechanism of cellulose hydrolysis catalyzed by cellulase Cel5A from Acidothermus cellulolyticus, J. Phys. Chem. B 114 (2010) 1462–1470.
[20] L. Petersen, A. Ardevol, C. Rovira, P.J. Reilly, Mechanism of cellulose hydrolysis by inverting GH8 endoglucanases: a QM/MM metadynamics study, J. Phys. Chem. B 113 (2009) 7331–7339.
[21] M.E.S. Soliman, J.J.R. Pernia, I.R. Greig, I.H. Williams, Mechanism of glycoside hydrolysis: a comparative QM/MM molecular dynamics analysis for wild type and Y69F mutant retaining xylanases, Org. Biomol. Chem. 7 (2009) 5236–5244.
[22] A. Bottoni, G. Pietro Miscione, M. Calvaresi, Computational evidence for the substrate-assisted catalytic mechanism of O-GlcNAcase. A DFT investigation, Phys. Chem. Chem. Phys. 13 (2011) 9568–9577.
[23] Ó. Passos, P. Fernandes, M. Ramos, Theoretical insights into the catalytic mechanism of β-hexosaminidase, Theor. Chem. Acc. 129 (2011) 119–129.
[24] E. Bokma, H.J. Rozeboom, M. Sibbald, B.W. Dijkstra, J.J. Beintema, Expression and characterization of active site mutants of hevamine, a chitinase from the rubber tree *Hevea brasiliensis*, Eur. J. Biochem. 269 (2002) 893–901.
[25] Y.C. Hsieh, Y.J. Wu, T.Y. Chiang, C.Y. Kuo, K.L. Shrestha, C.F. Chao, et al., Crystal structures of Bacillus cereus NCTU2 chitinase complexes with chitooligomers reveal novel substrate binding for catalysis: a chitinase without chitin binding and insertion domains, J. Biol. Chem. 285 (2010) 31603–31615.
[26] Y. Papanikolau, G. Prag, G. Tavlas, C.E. Vorgias, A.B. Oppenheim, K. Petratos, High resolution structural analyses of mutant chitinase A complexes with substrates provide new insight into the mechanism of catalysis, Biochemistry 40 (2001) 11338–11343.
[27] M. Umekawa, W. Huang, B. Li, K. Fujita, H. Ashida, L.-X. Wang, et al., Mutants of *Mucor hiemalis* endo-β-N-acetylglucosaminidase show enhanced transglycosylation and glycosynthase-like activities, J. Biol. Chem. 283 (2008) 4469–4479.
[28] J. Madhuprakash, K. Tanneeru, P. Purushotham, L. Guruprasad, A.R. Podile, Transglycosylation by chitinase D from *Serratia proteamaculans* improved through altered substrate interactions, J. Biol. Chem. 287 (2012) 44619–44627.
[29] H. Zakariassen, M.C. Hansen, M. Joranli, V.G. Eijsink, M. Sorlie, Mutational effects on transglycosylating activity of family 18 chitinases and construction of a hypertransglycosylating mutant, Biochemistry 50 (2011) 5693–5703.